STAR Note # 179
July 28, 1994
(revised Sept 16, 1994)

Resolving Overlapped Pairs of TPC Tracks Using Global Template Matching

Dhammika Weerasundara and Declan Keane
Kent State University

Abstract

We describe a template matching algorithm for extracting the momentum difference vector for a closely-spaced pair of tracks. The method enjoys the performance advantages of global tracking techniques such as Elastic Tracking while avoiding the difficulties that have so far prevented global tracking from being implemented as a practical alternative to conventional roadfinder tracking. The new algorithm offers good performance even when momentum differences q are too small and track momenta too large for conventional tracking, and is capable of attaining q resolutions on the order of 1 MeV/c, several times better than conventional tracking. This note describes proof-of-principle simulations in a simple geometry where complications caused by high multiplicities have been neglected. The crucial observable in our method is the width of the ionization trail, and the realism of this observable in the simulations has been verified by comparing with data from the EOS TPC. The next step will be fully realistic simulations for Au + Au events in STAR.

1 Introduction

We expect a central Au + Au collision at RHIC to result in 10^5 or more resolvable ionization clusters (hits) in the active volume of the STAR TPC, assuming that the FRITIOF code gives a realistic prediction of what will be observed. The TPC pad plane is designed to yield acceptable overall track reconstruction performance [1, 2] for such events using existing tracking software. However, improved tracking algorithms could offer many payoffs, such as better two-track resolution, reduced confusion and higher utilization of data near the inner part of the chamber, and a greater margin of protection against a sharp drop in performance if the real events turn out to be more challenging than the current simulations.

The existing STAR TPC tracking software [1] uses a variation of the conventional Road Finding (RF) algorithm, also known as the "follow-your-nose" method. RF tracking must be preceded by hitfinding — the step in which the centroids of all distinct clusters of ionization are calculated, and partially overlapping clusters are deconvoluted where possible. Then the tracking code operates on only the centroid and amplitude for each recognizable cluster. The RF algorithm searches for near-collinear track segments ("chains"), beginning at the outermost pad rows where track density is lowest, and these chains are extrapolated step-by-step from one local region of the detector to the next.

Global tracking sets out to circumvent two major shortcomings of the conventional approach: first, it eliminates preprocessing of the raw data (*e.g.*, hitfinding) and so retains the information normally lost during that stage of data reduction; second, it avoids the need to make many separate "decisions" based on information from small local regions of the active volume when tracks are being found. For example, the Elastic Tracking (ET) algorithm proposed by Gyulassy and Harlander [3, 4] uses the idea of sweeping template tracks across the detector and searching for the minimum in a function which reflects the overall discrepancy between the data and template over the entire trajectory. (Unfortunately, the term "global tracking" has recently been adopted in STAR to describe something completely different: the process of combining local tracking parameters from the TPC with information from other detector subsystems such as the SVT.) Global tracking has the potential [3, 4] to operate successfully in environments where track densities are several times higher than the limit where conventional RF methods become hopelessly confused. Nevertheless, global tracking has yet to be proven as a practical method for real-world high multiplicity data. A number of formidable difficulties were identified in a preliminary study [5] of Elastic Tracking in a two-dimensional simulation using EOS TPC geometry: the CPU time needed is about two orders higher than RF and that gap must inevitably widen for tracking in three dimensions; also it appears that even after minimizing the proposed ET function, Landau fluctuations can result in fitted trajectories that are systematically perturbed from the correct position.

In this note, we describe a strategy for tapping into some of the advantages of global tracking while still making full use of the tried-and-trusted RF method. We have chosen the case of track pairs that are too close in momentum to be resolved by conventional tracking; such pairs are of particular interest for interferometry analyses. Two-track resolution is particularly crucial along the direction of the average transverse momentum of the pair, since this carries information about the lifetime of the source. Lifetime information has possible importance as a plasma signature [6, 7, 8], but source radii larger than about 10 fm along the temporal direction probably cannot be resolved in STAR using conventional tracking [1, 2]. It is demonstrated below that even if the clusters associated with two almost overlapped tracks cannot be deconvoluted pair-by-pair using a hitfinder approach, the width of the merged clusters in the pad row direction (information that is invariably discarded by hitfinders) can be used in a template-matching procedure to resolve the relative momentum of the two tracks.

In the absence of a general-purpose implementation of global tracking, we rely on conventional tracking to identify candidates for the above procedure. There are several possible signatures for an RF chain that could be a double track. Simulations of dE/dx resolution in the STAR TPC indicate that candidates for overlapping $\pi^+\pi^+$ and $\pi^-\pi^-$ pairs could be preselected with useful efficiency using conventional tracking to find an (apparently) single track segment with momentum near $(\mathbf{p}_1 + \mathbf{p}_2)/2$ and with dE/dx near twice that of a pion with this momentum (see ref. [1], p. 4C-35). Another feasible approach is to look for TPC chains in a "Y" configuration, or pairs of SVT tracks that line-up with a single TPC track. It is not necessary for these initial selection criteria to have a high efficiency for rejecting single tracks. After double track candidates have been selected and subjected to a width template-matching (WTM) analysis as described in the following sections, any remaining single tracks (or irretrievably overlapped double tracks) can be rejected. Furthermore, the utility of the WTM method is not limited to track pairs where roadfinding cannot resolve the momentum difference, $\vec{q}$. WTM can offer improved $\vec{q}$ resolution for pairs where the RF technique is capable of providing an initial estimate of $\vec{q}$.

2 Monte Carlo Simulations

We envisage testing the performance of the WTM analysis for close pairs of tracks in two or more distinct phases. We begin in this note with a proof-of-principle Monte Carlo simulation for a simple TPC geometry in two dimensions (in the magnetic bend plane) with a multiplicity of two. Thus, for now we neglect possible complications from other tracks crossing the trajectory of the pair in question, and we assume that the above-mentioned procedures for identifying pair candidates will work satisfactorily. Although much work will be needed to implement WTM in the context of central Au + Au events in STAR, we believe that the present simulation addresses the important questions of utility and overall feasibility.

The current simulation includes the effect of multiple Coulomb scattering in the TPC gas. Multiple scattering in the material between the interaction vertex and the active volume of the STAR TPC is considered separately in section 4. For the sake of simplicity and to enable comparison with real data from the EOS TPC [9], we simulate a rectangular pad plane with 120 pads along the x direction and 128 pad rows along the z direction. Each pad has dimensions $\Delta x = 0.8$ cm and $\Delta z = 1.2$ cm, and the vertex is assumed to lie outside the active volume at $x = 0$ cm and $z = -81$ cm, where the origin is taken to lie at the center of the pad plane.

For this study, a sample of 11,400 pion pairs was generated within the following parameter space, with uniform density:

- Average momentum $\langle \vec{P} \rangle$ of the track pair ranged between 150 MeV/c and 950 MeV/c.
- Average angle $\langle \theta \rangle$ of the pair relative to the z axis ranged between 10° and 50°.
- Magnitude of the momentum difference vector $\vec{q}$ ranged between 3 MeV/c and 24 MeV/c.
- Angle α between $\langle \vec{P} \rangle$ and $\vec{q}$ ranged between 10° and 170° (where α increases counter-clockwise).

Monte Carlo track pairs were traced through the TPC along circular orbits assuming a 13 kG uniform magnetic field perpendicular to the pad plane, taking into account the geometrical acceptance of the TPC. The simulated ionization energy loss included full Landau fluctuations. The magnitude of the induced charge across each pad in a given pad row was calculated according to the track length projected over each pad. The spatial extent of the charge distribution across a pad row was calculated according to a Gaussian pad response function similar to the one being used for STAR TPC simulations [2]. The characteristic width of this pad response function is given by

$$\sigma_{\mathrm{prf}}^2 = \sigma_0^2 + \sigma_D^2 \lambda (1 + \tan^2 \alpha') + D^2 [\tfrac{1}{12} (\tan \alpha' - \tan \beta)^2 + S_2 \tan^2 \alpha'] \tag{1}$$

with drift distance λ set to 50 cm and σ_D^2 set to a value corresponding to a 13 kG magnetic field. All the other parameters have the values described in the STAR CDR update [2]. The pad signal amplitudes were converted to ADC counts by multiplying by 1000 and a threshold of 7 ADC counts was applied.

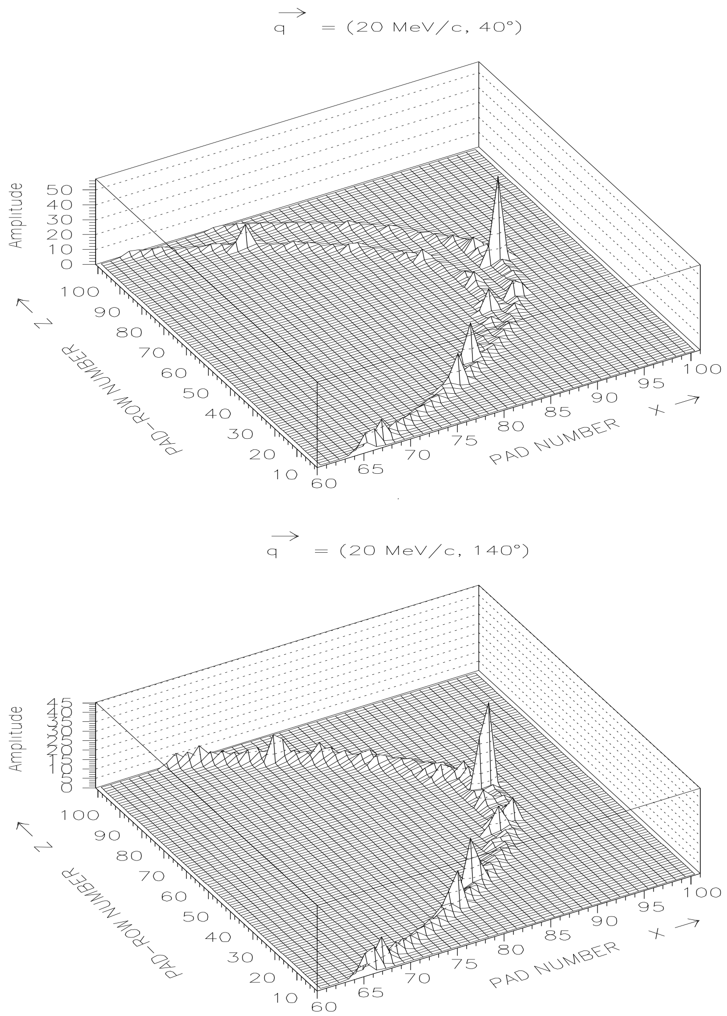

Figure 1: Simulated signal amplitudes for a pair of pions with $\langle \vec{P} \rangle = 400$ MeV/c, $\langle \theta \rangle = 40^\circ$ and momentum difference $q = 20$ MeV/c. The only difference between the upper and lower plots is in the sign of the component of $\vec{q}$ parallel to $\langle \vec{P} \rangle$. With conventional tracking, it would be impossible to resolve the track pair in the bottom plot.

Fig. 1 shows the distribution of signal amplitudes along the trajectory of the track pair specified in the caption. In the two parts of this figure, the magnitude of the momentum difference q is the same, and indeed, the only difference is in the sign of the component of q parallel to $\langle \vec{P} \rangle$; however, it is clear that changing the sign of $q_{||}$ has a dramatic effect on the ability of conventional local tracking to resolve the pair. The fact that the $\alpha = 140^\circ$ pair cannot be resolved using RF tracking is a consequence of an unfavorable interplay between the magnetic field and the two components of q, and is a potential source of distortion in interferometry studies.

The rms width $w(z_i)$ of the charge distribution on the ith pad row due to a low-q track pair is calculated as follows.

$$w^2(z_i) = \langle x^2 \rangle_i - \langle x \rangle_i^2 \tag{2}$$

with

$$\langle x^2 \rangle_i = \sum_j a_{ij} x_j^2 / \sum_j a_{ij} \,, \tag{3}$$

$$\langle x \rangle_i = \sum_j a_{ij} x_j / \sum_j a_{ij} \,, \tag{4}$$

where x_j is x coordinate at the center of the jth pad column, a_{ij} is the signal amplitude on the (i, j) pad, and the sums extend over an interval of j centered on the track pair. The selection of this interval is trivial in the context of the current simulation with multiplicity $= 2$, but this will not be the case in the future when dealing with realistic RHIC events. The corrected rms width is defined as $W = w/\sigma_{\rm prf}$. Hence $W(z_i)$ should be constant for a single track, since W is corrected for factors such as pad crossing angle and drift distance which can cause the width of clusters produced by a single track to vary from one pad row to another. We follow a truncation procedure similar to that used in processing dE/dx measurements: clusters whose amplitude lies in the uppermost 30% of the population are removed in order to minimize fluctuations in W.

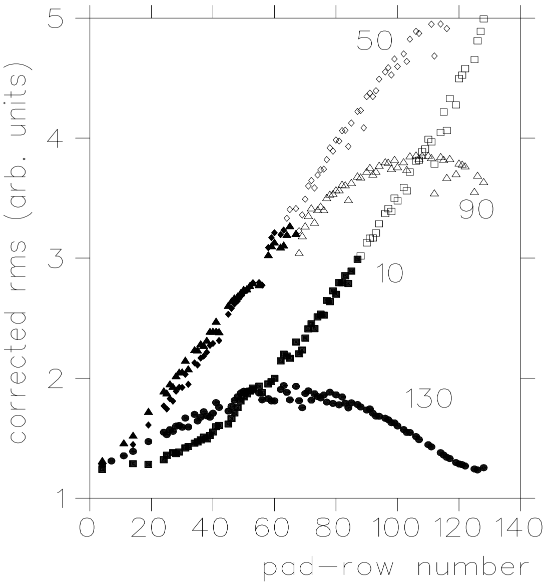

Figure 2: The variation of corrected rms width W along the trajectory of a pion pair with $\langle \vec{P} \rangle = 400$ MeV/c, $\langle \theta \rangle = 40°$, $q = 10$ MeV/c, and $\alpha = 10°$, $50°$, $90°$ and $130°$. The solid plot symbols indicate the regions where the two tracks are closer than 2 cm, leading to merged hits in the current TPC fast simulator.

It is observed that the variation of W along the trajectory of a track pair is a strong function of the vector $\vec{q}$ (see Fig. 2), and this dependence persists in regions of $\vec{q}$ where RF tracking cannot resolve the two tracks. This variation can be exploited to extract $\vec{q}$ from data. A procedure to extract $\vec{q}$ is described briefly in section 3.

It is important to verify that the distributions of w and W that we obtain from our TPC simulation are realistic. For this purpose, some comparisons have been made with EOS

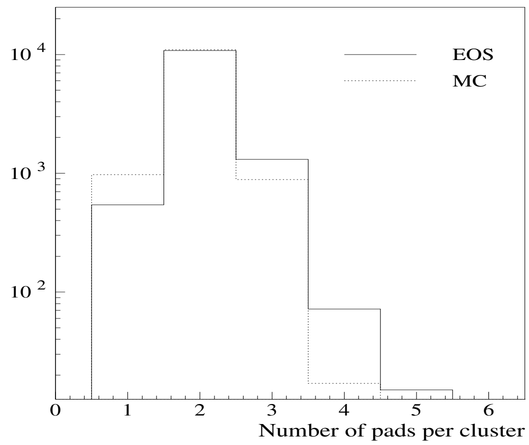

Figure 3: The distribution of number of pads per cluster above threshold, for a single track.

TPC data where the chamber was operated at low gain (below the threshold for detection of minimum ionizing particles) and triggered on single, non-interacting ^{58}Ni beam ions at momentum $730A$ MeV/c. These strongly ionizing tracks were chosen in part because in the normal mode of operation of EOS, near-minimum ionizing tracks generate a higher fraction of one-pad hits than in STAR. Fig. 3 shows the distribution of the number of pads per charge cluster. The solid line is for EOS TPC data and the dotted line is for our simulation. We expect the δ-ray production rate to be higher for a $Z = 28$ ion than for a singly-charged particle, although we must allow for the loss below threshold of some δ ionization due to reduced gain in EOS; thus part or all of the slightly broader distribution for EOS data might be attributable to the large charge of Ni. The reasonable overall agreement between data and simulations in Fig. 3 gives us confidence in the width information provided by the simulations.

3 Extracting $\vec{q}$

In this section, we demonstrate that an iterative procedure can be used to extract $\vec{q}$ from the simulated measurements of $W(z_i)$. $\vec{q}$ is represented by its magnitude q and its angle α relative to $\langle \vec{P} \rangle$, *i.e.*, $\vec{q} = (q, \alpha)$. First, a starting value $(q_{(\mu=0)}, \alpha_{(\nu=0)})$ is chosen from a look-up table, based on $\langle P \rangle$, $\langle \theta \rangle$, and $W(z_i)$. We scan for a minimum in the function

$$f = \sum_i [W(z_i) - W_{\mu,\nu}(z_i)]^4 \qquad (5)$$

where $W_{\mu,\nu}$ is the calculated width using the test value (q_μ, α_ν). We choose a sum of terms to the power of 4 rather than the more customary squared terms because this definition for f allows a satisfactory $\vec{q}$ to be found more quickly. In the first scan, the step sizes for q and α are set to 2 MeV/c and 2° respectively, and the search windows are set to $\pm$ 20 MeV/c and $\pm$ 20° respectively. The second iteration then uses the $\vec{q}$ corresponding to the minimum

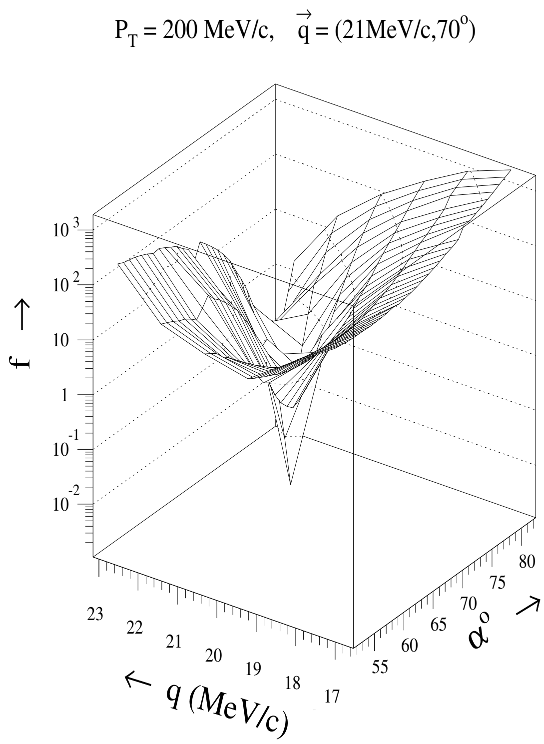

Figure 4: The quantity f, which is a minimum when the template matches the simulated width data, as a function of $\vec{q} = (q,\ \alpha)$.

f from the first round as its starting value, and searches again with smaller step sizes and narrower search windows. Fig. 4 demonstrates the variation of f in (q, α) space during the first iteration for a sample pion pair with $\langle \vec{P}\, \rangle = 400$ MeV/c and $\vec{q} = (21$ MeV/c, $70°)$. The minimum f occurs at $q = 21$ MeV/c and $\alpha = 73°$. The iterative procedure currently takes an average of 20 CPU-seconds per pair on a VAX 4090, but we believe that a substantial improvement in the computational efficiency of the code is possible.

4 $\vec{q}$ Resolution and Overall Performance

For the purpose of characterizing the performance of the WTM method, Fig. 5 presents simulated resolutions (*i.e.,* distributions of the input parameter for a pion pair minus the reconstructed value of that parameter) for q, α, $q_\perp$ and $q_{||}$; the latter two components are measured relative to the direction of $\langle \vec{P}\, \rangle$. The corresponding FWHM resolutions for these four parameters are ~ 2 MeV/c, $\sim 2°$, ~ 1 MeV/c and ~ 1 MeV/c, respectively. These resolutions are averaged over the full parameter space probed in the simulations, as specified in section 2. Even if a narrow region of this parameter space is selected, it is found that the q resolution distributions using WTM do not have the Gaussian shape observed in the case of conventional tracking.

We have not examined q resolution using RF tracking in the framework of the current simulations, so a comparison of the two methods using exactly the same criteria is not possible. In lieu of a direct comparison, we have tested the WTM method under conditions that come close to those used for the study of q resolution in the STAR CDR (p. 4C-37); in particular, we consider the same momentum region and use a similar number of samples. We obtain q resolutions using WTM that are at least 5 times better than the values quoted

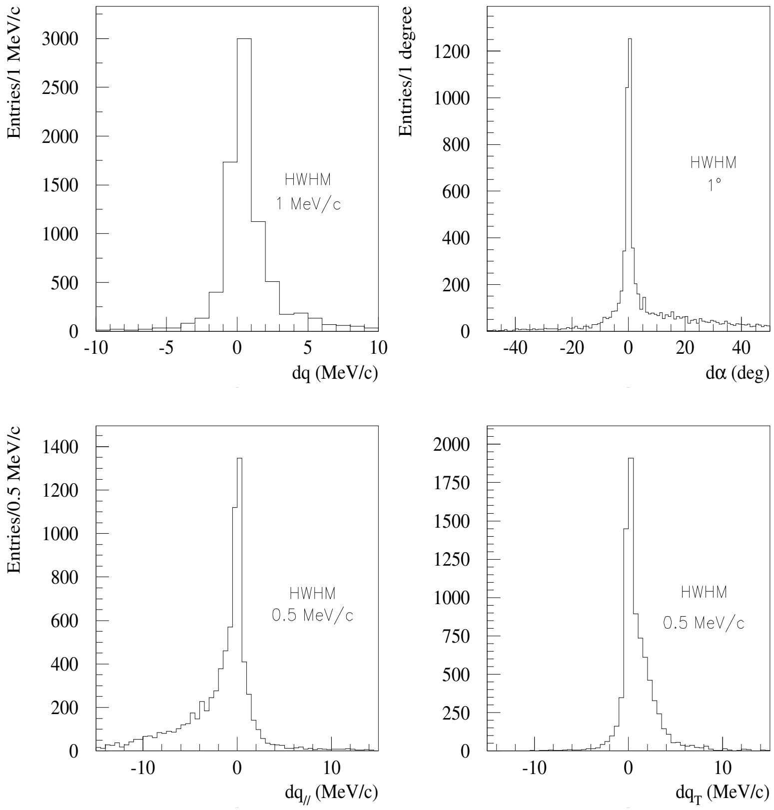

Figure 5: Difference between the input and reconstructed values for q, α, $q_\perp$ and $q_{||}$.

in the STAR CDR. A caveat that must be attached to this comparison is that multiple scattering in our WTM simulations only takes account of the TPC gas; for reasons discussed below, it is appropriate to separately consider the materials between the primary vertex and the TPC gas.

In conjunction with the above improvement in q resolution, the WTM algorithm also allows pairs with smaller q to be reconstructed. In the case of conventional tracking, we consider a pair to be adequately resolved if two-thirds or more of the clusters are separated by 2 cm or more, while the criteria in the case of the WTM method are $f < 1$ and $|dq| \leq 2$ MeV$/c$ and $|d\alpha| \leq 3°$. (We must employ completely different criteria because as already noted, we have not tested q resolution using RF tracking in the current simulations. However, the average q resolution for the accepted pairs using WTM is always better than that for the accepted pairs using our criteria for RF tracking.) Fig. 6 shows the relative density of pairs in the plane of q and $\langle \vec{P}\,\rangle$ after satisfying these criteria; panel (a) is for conventional tracking and (b) is for the WTM method. Perfect tracking would correspond to a uniform density over the entire plane above $\langle \vec{P}\,\rangle = 150$ MeV$/c$ and below $q = 25$ MeV$/c$. We see that the WTM method leads to a substantial broadening of the region where useful source parameters could be extracted.

Multiple Coulomb scattering in the material between the interaction vertex and the

STAR TPC places some restrictions on the utility of the new region of good q resolution opened up by the WTM method. Fig. 7 describes pion pairs in the plane of q and $\langle P \rangle$, showing contours labeled with the fraction of pairs having their q perturbed less than 10% by multiple Coulomb scattering. As discussed previously, the $q_{||}$ component carries the important information about the temporal extension of the source and is not directly affected by multiple scattering. However, it is necessary to subtract a transverse spatial term in quadrature in order to extract a source lifetime, and depending on the relative size of the terms, multiple scattering can seriously degrade the lifetime resolution. The SVT is the main source of MCS distortion in $q_{\perp}$ extracted from the TPC, but of course the SVT also offers the possibility to correct much of that distortion for matched tracks. Overall, it is reasonable to expect that at worst, multiple Coulomb scattering might limit the utility of WTM tracking in some parts of the newly accessible regions of Fig. 6.

As discussed in section 2, the simulations described in this note demonstrate the feasibility of WTM tracking in a simplified low-multiplicity environment. The next phase will involve simulations in a realistic high multiplicity environment with STAR materials and geometry.

This note describes the continuation of a research project started by John Harden as part of a Master's degree. We thank Marvin Justice for assistance at several stages of this work.

References

[1] STAR Conceptual Design Report, PUB-5347 (1992).

[2] STAR Project Conceptual Design Report Update (1993).

[3] M. Gyulassy and M. Harlander, Comp. Phys. Commun. **66**, 31 (1991).

[4] M. Gyulassy and M. Harlander, Nucl. Inst. and Meth. **A316**, 238 (1992).

[5] Marvin Justice, private communication and forthcoming STAR Note.

[6] S. Pratt, Phys. Rev. Lett. **53**, 1219 (1984).

[7] G. Bertsch, M. Gong, and M. Tohyama, Phys. Rev. C **37**, 1896 (1988).

[8] G. Bertsch and G. E. Brown, Phys. Rev. C **40**, 1830 (1989).

[9] G. Rai, A. Arthur, F. Bieser, C.W. Harnden, R. Jones, S. Kleinfelder, K. Lee, H.S. Matis, M. Nakamura, C. McParland, D. Nesbitt, G. Odyniec, D. Olson, H.G. Pugh, H.G. Ritter, T.J.M. Symons, H. Wieman, M. Wright, R. Wright, and A. Rudge, IEEE Trans. Nucl. Sci. **37**, 56 (1990).

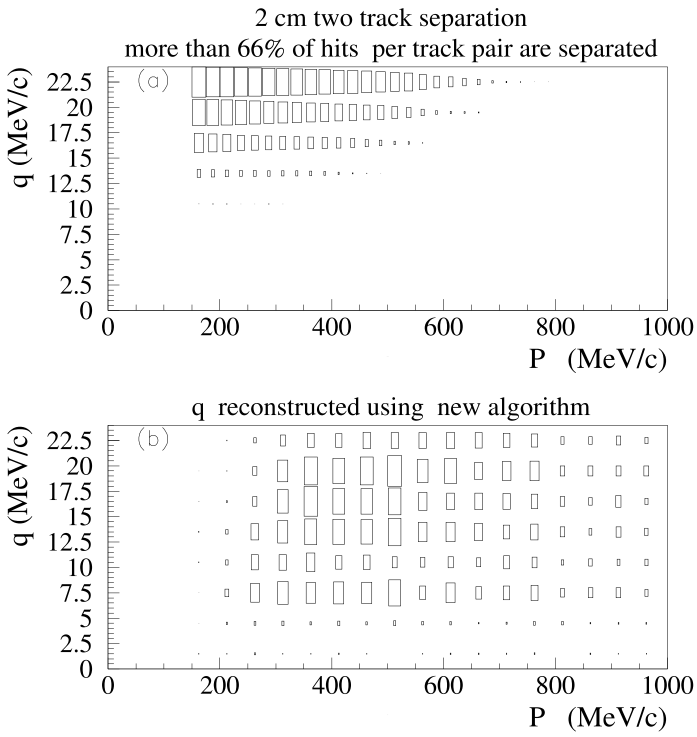

Figure 6: Relative pair-reconstruction efficiency as a function of mean momentum and momentum difference, (a) for conventional tracking, and (b) for the WTM method.

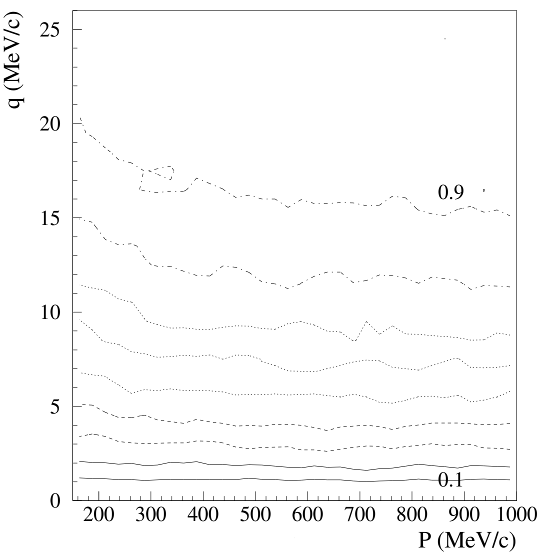

Figure 7: The usual plane of relative momentum versus mean pair momentum, showing contours labeled with the fraction of pairs having their q magnitude perturbed less than 10% by multiple Coulomb scattering in the material between the primary vertex and the active volume of the STAR TPC.